Dalton Transactions

ROYAL SOCIETY OF CHEMISTRY

PAPER

View Article Online
View Journal | View Issue

Cite this: *Dalton Trans.*, 2026, **55**, 5151

Expanding the reactivity of Rosenthal's reagent to cyclopropenes and allenes

Marcel Eilers, Dennis Geik, Marc Schmidtmann, Sven Doye and Rüdiger Beckhaus *

Received 9th January 2026,
Accepted 17th February 2026

DOI: 10.1039/d6dt00059b

rsc.li/dalton

The reactions of the Rosenthal reagent $Cp_2Ti(\eta^2$-BTMSA) with cyclopropenes and allenes were systematically investigated. With cyclopropenes, selective 1,2-insertion into the Ti–C bond induces a ring expansion from three- to five-membered frameworks, affording titanacyclopentenes. These bicyclic complexes undergo rearrangement under mild conditions to generate highly reactive titanium carbene species, which subsequently participate in [2 + 2] cycloaddition reactions with alkynes (BTMSA and 1,2-diphenylacetylene), yielding titanacyclobutenes. In contrast, reactions with allenes proceed *via* ligand exchange of the alkyne ligand, giving titanacyclopentane derivatives. In addition to these transformations, the titanium complex was found to catalyze the isomerization of cyclotrideca-1,2-diene to cyclotrideca-1,3-diene. All isolated complexes were comprehensively characterized by NMR spectroscopy, and the solid-state structures of most species were identified by single-crystal X-ray diffraction.

Introduction

Olefin complexes of early transition metals have been of considerable interest in organometallic chemistry for many years, largely due to their key roles in many transformations, including polymerization[1] as well as metathesis reactions.[2] Seminal work by Bercaw and co-workers established olefin complexes as crucial intermediates in such processes (Fig. 1, **I**), while the introduction of sterically demanding Cp* ligands (Cp* = pentamethylcyclopentadienyl) subsequently enabled the isolation of discrete and well-defined examples.[3]

Beyond simple olefins, allenes and cyclopropenes were also shown to coordinate in an η^2 fashion (Fig. 1, **II** and **III**). Binger and co-workers reported several pioneering examples of η^2-cyclopropene and η^2-allene titanium complexes.[4–6] The direct attempts to generate the corresponding titanacyclopentanes (**IV**) from ethylene were often unsuccessful, primarily due to rapid decomposition accompanied by the release of ethylene.[7] Binger's group achieved the isolation of substituted titanacyclopentanes (Fig. 1, **V** and **VI**) from the reaction of $Cp_2Ti(PMe_3)_2$ with allenes and cyclopropenes, thereby establishing important precedents for controlled C–C bond formation at low-valent titanium centers.[4–6] Driven by the need for reliable low-valent group 4 metal sources, metallocene-based Ti^{II} and Zr^{II} complexes subsequently emerged as powerful tools in organometallic synthesis. Prominent among these are bis(trimethylsilyl)acetylene (BTMSA) adducts, commonly referred to as "Rosenthal complexes" (*e.g.* $Cp_2Zr(L)(\eta^2$-BTMSA) or $Cp_2Ti(\eta^2$-BTMSA); L = pyridine or THF). These compounds act as masked Ti^{II} or Zr^{II} sources, releasing highly reactive low-valent fragments under mild conditions through simple ligand dissociation (Scheme 1, top).[8,9]

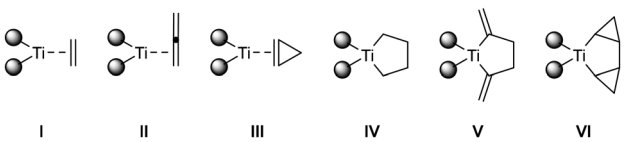

Fig. 1 Simplified structures of titanium olefin complexes (**I–III**) and titanacyclopentane complexes (**IV–VI**).

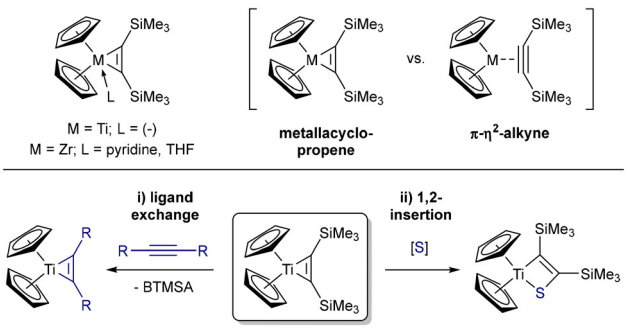

Scheme 1 Rosenthal's reagents (top) as Cp_2Ti^{II} and Cp_2Zr^{II} synthons in ligand exchange and 1,2-insertion reactions (bottom).

Institut für Chemie, Carl von Ossietzky Universität Oldenburg, Postfach 2503, 26111 Oldenburg, Germany. E-mail: ruediger.beckhaus@uni-oldenburg.de

The resulting Cp_2M^{II} fragments represent versatile platforms for the straightforward construction of structurally diverse titanium and zirconium complexes and have been employed in various C–C bond-forming reactions, as well as catalytic transformations.[8,10] Notably, Cp_2Ti^{II} species may also undergo oxidation reactions to form Cp_2Ti^{III} complexes, either through comproportionation,[11] *via* reaction with metal salts such as AgOTf (with concomitant formation of Ag^0), or through protonation accompanied by H_2 evolution.[12] The two fundamental elementary reactions of Rosenthal complexes are (i) ligand exchange involving the BTMSA ligand and (ii) 1,2-insertions of unsaturated substrates [S] into the three-membered titanium ring system (Scheme 1, bottom). The sequence of reactions may vary depending on the substrate and the transition metal, with 1,2-insertion sometimes occurring prior to ligand substitution.[8] Cumulated π-systems have been investigated extensively, for example by the groups of Burlakov,[13] Rosenthal,[14,15] Tonks,[16] and Beweries.[17] In particular, the synthesis of stable 1-metallacyclobuta-2,3-dienes has demonstrated how Cp_2M^{II} fragments can engage in cyclization reactions with cumulated systems.[18] Likewise, carbodiimides have been studied in detail both experimentally and theoretically, providing pathways to Arduengo-type carbene complexes including a new type of heterocumulene coordination mode.[14–16]

Despite this breadth of reactivity, systematic studies on the interaction of cyclopropenes and allenes with Ti^{II} centers remain scarce. Allenes, with their unique electronic distribution and potential for regio- and stereodivergent activation, and cyclopropenes, which combine significant ring strain with partial cumulated character, are particularly underexplored in the coordination sphere of Ti^{II} complexes. Notably, Binger and co-workers reported first investigations into the reactivity of both allenes and cyclopropenes with the related complex $Cp_2Ti(PMe_3)_2$.[4,6] Insights from related transformations, such as cumulene activation and metallacyclocumulene formation, suggest intriguing mechanistic pathways, including metallacyclopentadiene intermediates, ring-opening processes, and novel insertion modes. Herein, we report the reactivity of $Cp_2Ti(\eta^2$-BTMSA) **1** with cyclopropenes and allenes, providing new insights into the interaction of Ti^{II} centers with strained and cumulated π-systems and enabling selective C–C bond formation through controlled substrate activation.

Results and discussion

Reaction of 1 with cyclopropenes

The cyclopropenes were prepared in accordance with published procedures,[19] and after purification by chromatography or distillation, were degassed and stored under inert atmosphere at −30 °C. Reactions of $Cp_2Ti(\eta^2$-BTMSA) **1** with cyclopropenes **a–d** in *n*-hexane at ambient temperature led to an immediate colour change of the solution from yellow to deep purple, accompanied by the precipitation of purple solids. After one hour of stirring, the supernatant was removed, and the residue was washed with small portions of *n*-hexane and dried under high vacuum. The resulting complexes **2a–d** were obtained as purple solids in good isolated yields (67–87%, Scheme 2). They exhibit limited solubility in *n*-hexane but dissolve readily in aromatic solvents (toluene, benzene) or THF, and decompose in the solid state upon heating above 117 °C.

Product formation in these reactions was found to be independent of the stoichiometry. Accordingly, substoichiometric amounts of cyclopropenes led to incomplete conversion with unreacted complex **1** remaining, whereas the use of an excess did not affect the outcome. However, Binger and co-workers reported on additional insertion reactions under related conditions, resulting in the formation of titanacyclopentanes.[4] The selective formation of single products in the present case was confirmed by NMR spectroscopy. For example, the ^{1}H NMR spectrum of **2a** exhibits two singlets for the $SiMe_3$ groups at δ = 0.06 and 0.10 ppm, and two singlets for the Cp ring protons at δ = 5.83 and 5.91 ppm, the latter consistent with restricted rotation at the titanium center, indicating an asymmetric coordination environment in solution. A singlet at δ = 1.65 ppm is assigned to the methyl substituent of the cyclopropane moiety. In addition, the methine protons of the cyclopropane ring appear as doublets at δ = 1.45 and 1.73 ppm (J = 8.4 Hz). The structures of **2a–d** were further corroborated by single-crystal X-ray diffraction. Single crystals suitable for X-ray analysis were obtained by slow evaporation of concentrated *n*-hexane solutions at ambient temperature. The molecular structure of **2b** is depicted in Fig. 2, while those of **2a**, **2c**, and **2d** are provided in the SI. The solid-state data reveal the presence of two distinct molecular orientations within the unit cell, in which complexes **2a–d** adopt either a supine or a prone conformation.[20] These two orientations correspond to inversely oriented arrangements of the ligand framework, indicat-

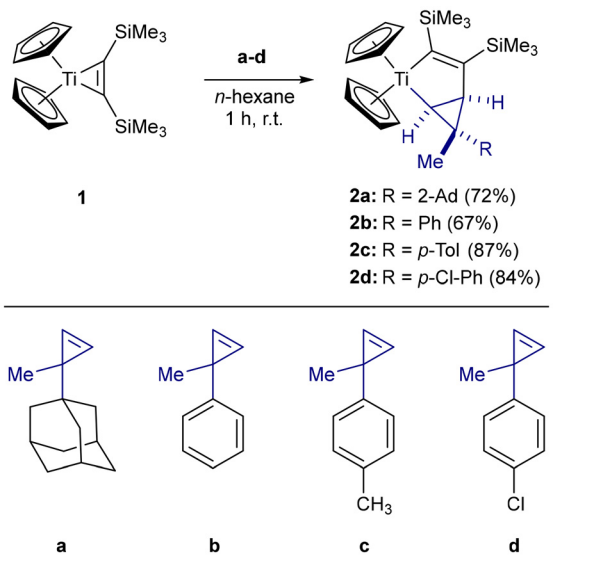

Scheme 2 Formation of bicyclic titanacyclopentene complexes **2a–d** from the reaction of $Cp_2Ti(\eta^2$-BTMSA) **1** with cyclopropenes **a–d** *via* 1,2-insertion.

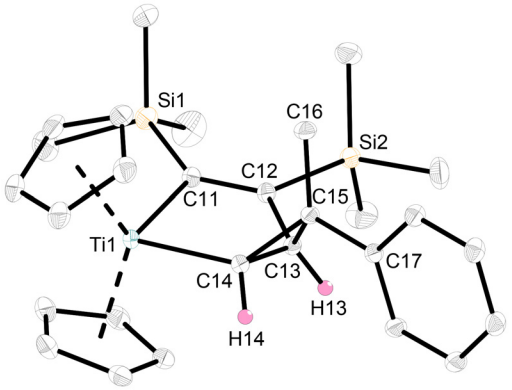

Fig. 2 Molecular structure of the supine isomer of complex **2b**. Thermal ellipsoids are drawn at the 50% probability level. Hydrogen atoms (except for H13 and H14) and the prone isomer are omitted for clarity.

ing that the complexes crystallize in two well-defined but opposing conformers. Notably, in both conformations the methyl group and the hydrogen atoms consistently adopt a *trans* configuration (Fig. S99–S102). We attribute this high selectivity primarily to steric effects in the transition state of cyclopropene incorporation. The Cp ligands and the methyl groups of the trimethylsilyl substituents are creating a sterically congested environment on both faces of the metallacycle.

To minimize steric repulsion, the smaller methyl substituent of the cyclopropene is preferentially oriented toward this hindered region, whereas the bulkier groups are directed away from it, resulting in the exclusive formation of a single observable isomer. The molecular structure of **2b** reveals a distorted tetrahedral coordination geometry at the titanium center and shows cyclopropene insertion through formation of a new C12–C13 bond (1.5117(9) Å). The resulting titanacyclopentene deviates from planarity due to the sp^3 hybridization of the former cyclopropene carbons C13 and C14. The Ti1–C11 (2.1920(7) Å) and Ti1–C14 (2.1495(7) Å) bond lengths are slightly elongated compared to the sum of the covalent radii ($\sum r_{cov}$(Ti–C): 2.11 Å),[21] and are consistent with reported Ti–C bonds (2.22 Å).[22] Within the cyclopropane fragment, the C–C bond lengths (C13–C14: 1.5192(9) Å, C14–C15: 1.5349(9) Å, C13–C15: 1.5416(9) Å) are modestly elongated relative to typical C(sp^3)–C(sp^3) single bonds in unstrained cyclopropanes (1.51 Å).[23] Table 1 summarizes the bond lengths and angles of complexes **2a–d**, which exhibit comparable structural features. With extended reaction times, a subsequent transformation of **2a–d** was observed. At ambient temperature this process proceeds slowly and can be monitored by NMR spectroscopy; heating NMR samples (C_6D_6) to 60 °C for 24 h accelerated the

Table 1 Selected bond lengths (Å) for complexes **2a–d**

Complex	Ti1–C11	Ti1–C14	C11–C12	C12–C13	C13–C14	C13–C15	C14–C15	C11–Ti1–C14
2a	2.2037(9)	2.1392(9)	1.3662(13)	1.5099(13)	1.5267(13)	1.5442(12)	1.5204(12)	83.72(3)
2b	2.1920(7)	2.1495(7)	1.3640(9)	1.5117(9)	1.5192(9)	1.5416(9)	1.5349(9)	86.49(3)
2c	2.1911(5)	2.1423(5)	1.3645(7)	1.5120(6)	1.5186(7)	1.5469(7)	1.5291(7)	87.048(18)
2d	2.1903(6)	2.1445(6)	1.3667(8)	1.5134(8)	1.5159(8)	1.5469(8)	1.5299(8)	86.58(2)

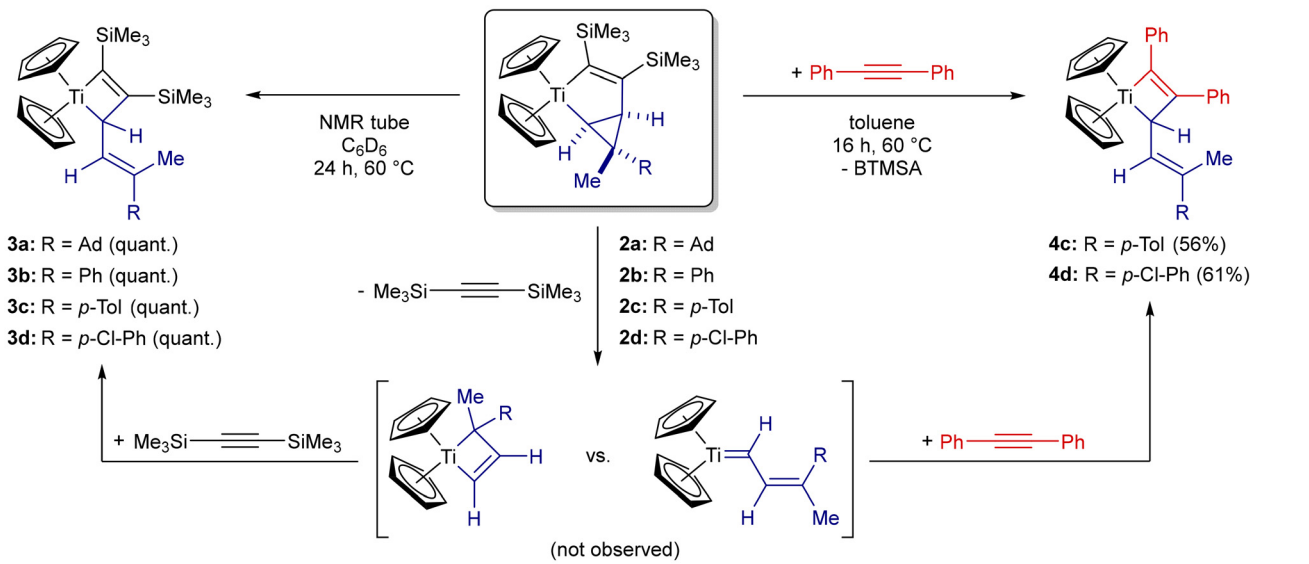

Scheme 3 Ring-opening of **2a–d** to titanium carbene intermediates and subsequent [2 + 2] cycloadditions with alkynes yielding titanacyclobutenes **3a–d** and **4c,d**.

conversion, accompanied by a distinct colour change from purple to orange (Scheme 3). The ^{1}H NMR spectra of complexes **2a–d** display new characteristic resonances that are consistent with the structural reorganization. Taking complex **3a** as a representative example, the former cyclopropane methine doublets at δ = 1.45 and 1.73 ppm are shifted downfield to δ = 5.91 and 6.07 ppm with a slightly increased coupling constant (J = 9.4 Hz), indicative of significant electronic changes within the ring system. Correspondingly, the ^{13}C NMR spectrum shows resonances for the methine carbons at δ = 123.8 and 135.6 ppm, which are consistent with a change in hybridization from sp^3 to sp^2. The quaternary carbons of the BTMSA moiety also shift from δ = 159.8 and 231.5 ppm to δ = 107.0 and 250.9 ppm. Additionally, the ^{29}Si NMR signals shift from δ = −20.3 and −14.4 ppm to δ = −13.8 and 1.1 ppm, as a result of the ring contraction. Additional changes in the ^{1}H NMR spectra include the methyl resonance (from δ = 1.29 to 1.75 ppm) and slight upfield shifts of the Cp resonances (from δ = 5.94, 5.97 to 5.27, 5.32 ppm). Related titanacyclopentene complexes have been shown to undergo facile ligand dissociation, thereby promoting C–C bond activation in the absence of steric shielding at the α-position.[5,24] We attribute the observed rearrangement to a ring-opening process that generates highly reactive titanium carbene intermediates *in situ*. While analogous processes are well established for ruthenium carbenes in ring-opening metathesis polymerization (ROMP),[25] direct observation of titanium carbene species remains challenging.[4] Previously, we reported titanavinylidene complexes that readily undergo formal [2 + 2] cycloadditions with alkynes.[26] Similarly, we propose that the transient titanium carbene complexes react with the liberated BTMSA ligand to afford titanacyclobutene complexes **3a–d**. In line with this hypothesis, heating **2c** and **2d** in the presence of 1,2-diphenylacetylene (60 °C, 16 h) resulted in a colour change of the solution from purple to green, and the corresponding cycloadducts **4c** and **4d** were isolated in 56–61% yield (Scheme 3).

The complexes exhibit good solubility in *n*-hexane, toluene, and benzene and decompose in the solid-state upon heating above 122 °C. NMR spectroscopy readily reveals the selective substitution of BTMSA by 1,2-diphenylacetylene. Although both alkynes are present in the reaction mixture, 1,2-diphenylacetylene is clearly preferred, as indicated by the ^{1}H NMR spectrum (see Fig. S39). New aromatic resonances corresponding to complex **4d** appear at δ = 6.84–7.24 ppm. The quaternary carbons of the incorporated 1,2-diphenylacetylene are observed at δ = 103.2 and 213.1 ppm in the ^{13}C{^{1}H} NMR spectrum. The methine proton doublets at δ^{1}H = 5.37 and 6.74 ppm (J = 9.7 Hz) are comparable to those of complex **3d** (δ^{1}H = 6.06 and 6.61 ppm, J = 10.1 Hz), supporting structural similarity of the central metallacycle.

The formation of complexes **3** and **4** was further corroborated by single-crystal X-ray diffraction. Single crystals of **4c** and **4d** suitable for X-ray analysis were obtained from concentrated benzene-d_6 and *n*-hexane solutions by slow evaporation at ambient temperature. The solid-state structures unambiguously

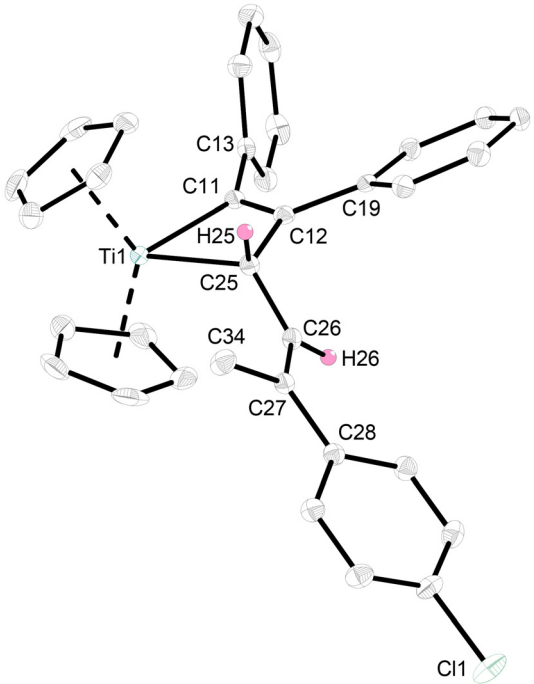

Fig. 3 Molecular structure of the prone isomer of complex **4d**. Thermal ellipsoids are drawn at the 50% probability level. Hydrogen atoms (except for H25 and H26) and the supine isomer are omitted for clarity.

confirm the formation of titanacyclobutenes and the substitution of BTMSA by 1,2-diphenylacetylene, consistent with NMR spectroscopic data. The molecular structure of **4d** is shown in Fig. 3, while the structure of **4c** is provided in the SI. The solid-state data also reveal the presence of both supine and prone conformations within the unit cell (see Fig. S103 and S104).[20]

The molecular structures of **4c** and **4d** reveal a distorted tetrahedral coordination environment at the titanium center, defined by two η^5-cyclopentadienyl ligands and one bidentate ligand. The exocyclic C–C bonds are slightly shortened compared to typical C–C single bonds (**4c**: 1.4736(11) Å; **4d**: 1.4729(18) Å).[21,23] The newly formed C–C bonds within the titanacyclobutene ring are elongated single bonds (**4c**: 1.5364(11) Å; **4d**: 1.5371(18) Å), yet notably shorter than the corresponding bond in a related complex reported by Tebbe *et al.* (1.598(5) Å).[27] In that work, the bonding situation was described as a titanium–methylene–acetylene adduct with a substitution-labile BTMSA ligand, formed *via* [2 + 2] cycloaddition between *in situ* generated titanium carbene species and BTMSA. This mechanism of carbene formation and subsequent cycloaddition with olefines and alkynes has also been also widely explored by Grubbs *et al.*[28]

The exocyclic C13–C14/C26–C27 bonds (**4c**: 1.3518(11) Å; **4d**: 1.3502(19) Å) exhibit double bond character when compared to the sum of the covalent radii ($\sum r_{cov}$(C–C): 1.34 Å)[29] and typical C=C double bonds (1.34 Å).[23] The resulting four-membered rings of **4c** and **4d**, composed of atoms Ti1, C11, C12, and C13/C25, are slightly puckered due to the sp^3 hybridization of the carbon atom of the former cyclopropane moiety. Accordingly, these sp^3-hybridized carbon atoms deviate from

Table 2 Selected bond lengths (Å) and angles (°) of complexes **4c** and **4d**

Complex	Ti1–C11	Ti1–C13/Ti1–C25	C11–C12	C12–C13/C12–C25	C13–C14/C25–C26	C14–C15/C26–C27	C11–Ti1–C13/C11–Ti1–C25
4c	2.1104(8)	2.1763(8)	1.3511(11)	1.5364(11)	1.4736(11)	1.3518(11)	69.97(3)
4d	2.1099(13)	2.1882(13)	1.3476(19)	1.5371(18)	1.4729(18)	1.3502(19)	69.32(5)

the mean plane by approximately 2.7° (**4c**) and 4.2° (**4d**). The Ti–C bond lengths (avg. 2.11 Å) are in line with expected values for titanium carbon single bonds ($\sum r_{cov}$(Ti–C): 2.11 Å),[21] and are consistent with those observed in complexes **2a–d** (avg. 2.12 Å). Table 2 summarizes the bond lengths and angles of complexes **4c** and **4d**.

Reaction of 1 with allenes

The allenes were either obtained from commercial suppliers (for **b** and **j**) or prepared according to literature procedures.[30] After purification by chromatography or distillation, the allenes were degassed and stored at −30 °C under inert conditions without decomposition. Reactions of $Cp_2Ti(\eta^2$-BTMSA) **1** with allenes **a–m** were carried out in *n*-hexane at ambient temperature (Scheme 4). Upon addition, the reaction mixtures immediately changed colour from yellow to red, and red precipitates formed (except **5c** and **5d**, which were isolated as red oils). After stirring for 1 h, the supernatant was decanted, and the residue was washed with a small amount of *n*-hexane and dried under high vacuum. The resulting complexes **5a–m** were obtained in yields of 28–96%. With the exception of **5c** and **5d**, the complexes exhibit limited solubility in *n*-hexane but dissolve readily in aromatic solvents (toluene, benzene) or in THF. In the solid state, they decompose upon heating above 117 °C.

Unlike the results reported by Binger *et al.*, the product formation was independent of stoichiometry and unaffected by the presence of PMe_3.[6] In the reaction of **1** with the parent allene propa-1,2-diene **a**, stirring for 15 minutes at ambient temperature followed by work-up initially yielded traces of the 2,4-dimethylene-1-titanacyclopentane complex as a minor side product (see Fig. S51). In solution, this species gradually converts into the 2,5-dimethylene-1-titanacyclopentane complex **5a** within one hour, indicating cleavage of the newly formed C_B–C_C bond and subsequent dissociation and reorganization within the titanium coordination sphere at ambient temperature. Formation of this side product has also been reported by Binger *et al.* for the corresponding zirconium complex; however, in that case no further transformation was observed.[6] In the ^{1}H NMR spectrum of **5a**, the product could be clearly identified as the titanacyclopentane complex. In addition to the singlet for the Cp protons at δ = 5.97 ppm, the CH_2 protons of the newly formed bridging C_B–C_C bonds in the ring system give a single signal at δ = 2.48 ppm, while the chemically inequivalent alkene protons at C_E and C_F resonate at δ = 3.45 and 5.38 ppm. These data indicate a symmetrical coordination environment at the titanium center. Single crystals of **5a** were obtained from a concentrated *n*-hexane solution at ambient temperature by slow evaporation. Single-crystal X-ray analysis confirmed the formation of the titanacyclopentane complex, consistent with the spectroscopic data. The molecular structures of **5a** and **5e** are shown in Fig. 4, with the structures of **5b** and **5i–l** being provided in the SI.

NMR spectroscopy and single-crystal X-ray diffraction demonstrate that the reaction of **1** with mono-substituted allenes **b–h** predominantly furnishes (*E*,*E*)-titanacyclopentane products (see Fig. 4, bottom). In the case of methoxyallene **b**, however, trace amounts of an additional 2,5-substituted (*E*/*Z*)-configured isomer **5b′** are observed, as evidenced by weak

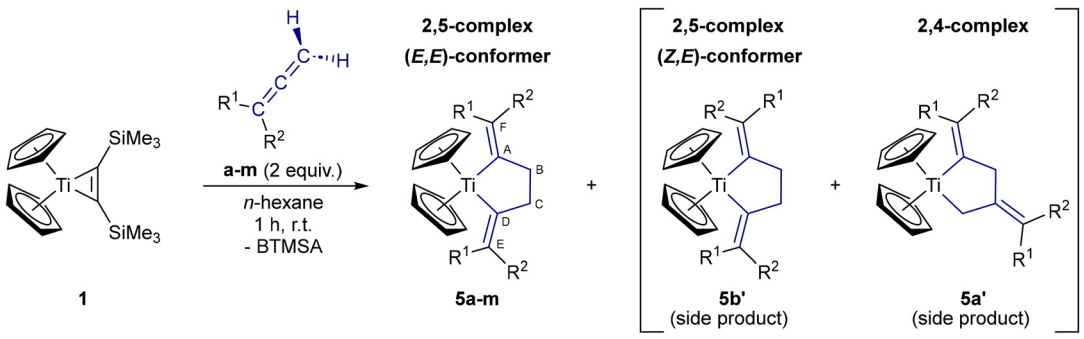

	R^1	R^2	Yield
5a	H	H	83%
5b	H	OMe	80%
5c	H	$CH_2Si(Me)_3$	28%
5d	H	C_6H_{13}	93%

	R^1	R^2	Yield
5e	H	Ph	56%
5f	H	Bn	86%
5g	H	$CH_2CH(C_6H_5)_2$	90%
5h	H	$CH_2CH(C_6H_4F)_2$	94%

	R^1	R^2	Yield
5i	Me	Ph	71%
5j	Me	Me	96%
5k	Cy	Cy	34%
5l	Ph	Ph	82%
5m	Bn	Bn	84%

Scheme 4 Formation of titanacyclopentane complexes **5a–m** from $Cp_2Ti(\eta^2$-BTMSA) **1** and allenes **a–m** *via* ligand substitution.

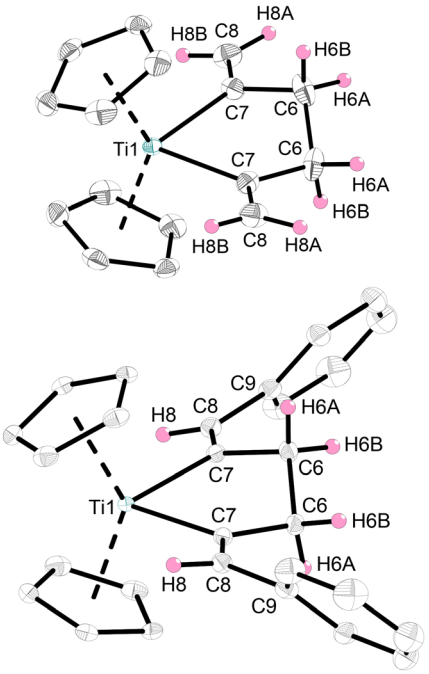

Fig. 4 Molecular structures of complexes **5a** (top) and **5e** (bottom). Thermal ellipsoids are drawn at the 50% probability level. Most hydrogen atoms are omitted for clarity.

additional signals in the ^{1}H NMR spectrum (Fig. S55). This minor species does not undergo further isomerisation over time in solution, in contrast to complex **5a**.

Reactions with disubstituted allenes **i–m** likewise furnished titanacyclopentane complexes, including those derived from sterically demanding substrates. The solid-state structures of selected products corroborate these findings and reveal that bulkier substituents adopt conformations oriented away from the titanium center. Significant bond lengths and angles of complexes **5a–5k** are summarized in Table 3, highlighting the influence of sterically demanding substituents on the bonding parameters. Collectively, these results demonstrate the generality of the titanium-mediated allene cyclization and provide insight into the stereochemical preferences governing the formation of the resulting metallacycles.

We next investigated the reactivity of **1** toward cyclic allenes. Owing to the inherent ring strain and constrained geometry of these substrates, particularly in the case of cyclotrideca-1,2-diene, the enforced distortion of the cumulated π-system significantly destabilizes the allene framework. Consequently, simple coordination to the metal center is expected to provide a favourable interaction that partially compensates for this destabilization, whereas additional C_B–C_C bond formation would further increase structural distortion and should therefore be disfavoured. The reaction of **1** with allenes **n–s** proceeded smoothly under mild conditions to afford the corresponding titanacyclopentane complexes **5n–s** in good to excellent yields (Scheme 5). As observed previously, product formation remained independent of stoichiometry. NMR spectroscopy revealed selective formation of single products, with no evidence of side reactions or isomerization. Single crystals suitable for X-ray analysis were obtained for several complexes, and the resulting structures confirmed the spectroscopic assignments. For instance, the molecular structure of **5r** is shown in Fig. 5 (top), while those of **5n**, **5o** and **5p** are provided in the SI. These results demonstrate that even strained cyclic allenes **n–s** undergo efficient titanium-mediated cyclization, underscoring the generality of this transformation and extending its scope to conformationally restricted systems.

A comparison of the bond lengths and angles (Table 4) reveals only a slight increase in the Ti–C_A and Ti–C_D bond distances, from 2.19 to 2.21 Å, consistent with the increased steric demand of the allene substituents. This is accompanied by a notable decrease in the C_A–Ti–C_D bond angles, which narrows from 86.8 to 78.4°. The C_B–C_C bond lengths fall within the range of elongated C–C single bonds compared to the sum of covalent radii, reaching up to 1.54 Å. The C_A–C_F and C_D–C_E double bonds are slightly elongated across the series, with complex **5p** displaying the longest values (1.35 and 1.36 Å) and **5t** the shortest (1.34 and 1.32 Å). In the molecular structures of complexes **5r** and **5t**, the corresponding ring systems of the former allenes adopt a *trans* configuration (Fig. 5).

The reaction of **1** with allene **t** was only successful when the cyclic allene was added directly to complex **1**. In this case, the formation of **5t** proceeded significantly more slowly than with the other allenes and did not afford a single, selective product. The formation of complex **5t′** as a side product was observed in the ^{1}H NMR spectra. In contrast to **5t**, which displays two distinct Cp resonances indicative of a sterically constrained environment that renders the Cp rings chemically inequiva-

Table 3 Selected bond lengths (Å) and angles (°) of complexes **5a**, **5b**, **5e**, **5f**, and **5i–k**

Complex	Ti–C_A	Ti–C_D	C_A–C_B	C_A–C_F	C_B–C_C	C_C–C_D	C_D–C_E	C_A–Ti–C_D
5a	2.1787(7)	2.1787(7)	1.5128(11)	1.3386(10)	1.4736(11)	1.5128(11)	1.3386(10)	81.74(4)
5b	2.1687(16)	2.1573(15)	1.524(2)	1.329(2)	1.541(3)	1.516(2)	1.336(2)	81.51(6)
5e	2.1813(7)	2.1813(7)	1.5158(10)	1.3490(10)	1.5380(14)	1.5158(10)	1.3490(10)	81.04(4)
5f	2.173(3)	2.166(3)	1.519(4)	1.339(4)	1.536(5)	1.522(4)	1.343(4)	82.14(11)
5i	2.1824(6)	2.1857(6)	1.5250(9)	1.3471(9)	1.5323(10)	1.5251(9)	1.3466(9)	84.87(2)
5j	2.1790(12)	2.1780(12)	1.5256(17)	1.3427(16)	1.5329(18)	1.5261(17)	1.3439(17)	86.79(4)
5k	2.2112(11)	2.2006(10)	1.546(2)	1.3492(14)	1.517(3)	1.525(2)	1.3465(14)	87.09(4)

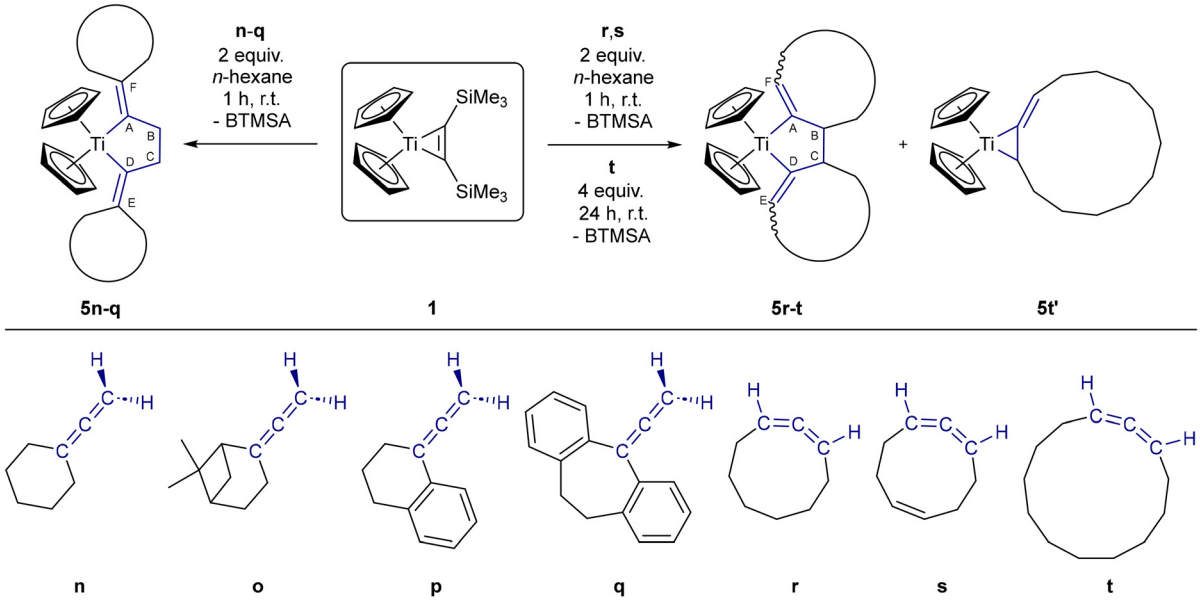

Scheme 5 Reaction of **1** with allenes **n**–**t** to afford titanacyclopentane complexes **5n**–**t** through ligand exchange and C–C bond formation.

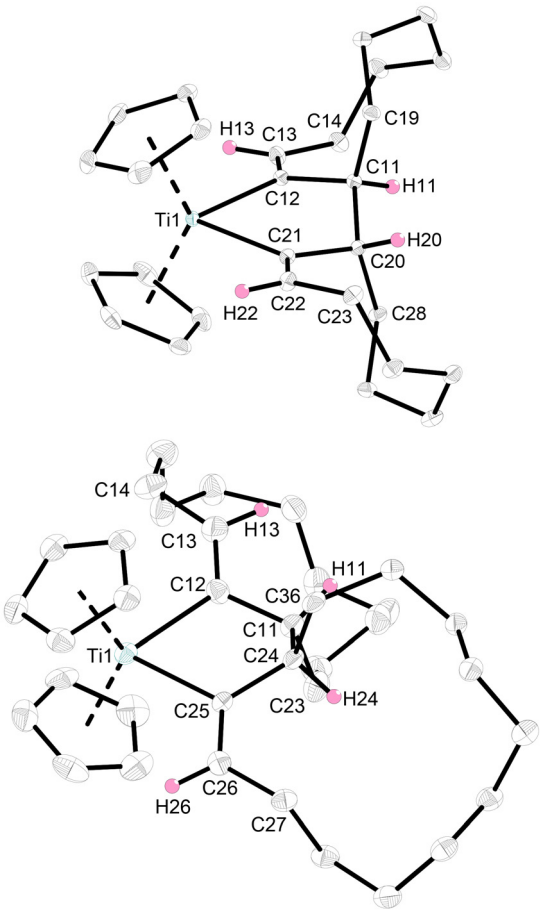

Fig. 5 Molecular structures of complex **5r** (top) and **5t** (bottom). Thermal ellipsoids are drawn at the 50% probability level. Only one of six crystallographically independent molecular structures of **5r** and only one of two crystallographically independent molecular structures of **5t** are shown. Most hydrogen atoms are omitted for clarity.

lent, complex **5t′** exhibits only a single Cp signal. Notably, in **5t** one CH_2 resonance of the Cp_2Ti-alkyl fragment is shifted markedly upfield (δ = −0.10 ppm). This pronounced high-field shift indicates an unusual magnetic environment in close proximity to the titanium center. In addition, one of the alkene protons in **5t** is shifted significantly downfield, appearing at 5.47 ppm (compared to approx. 3.5 ppm in complexes **5a**–**5r**), while the second alkene proton resonates between 1.20–2.20 ppm. These distinct chemical shift differences indicate a highly anisotropic proton environment. Examination of the single-crystal structure of **5t** (Fig. 5, bottom) reveals that the steric demand of the tridecene ring forces the alkene protons into unequal spatial orientations relative to the titanium center (*E* and *Z* configuration). The proton H26 oriented toward the metal center may experience pronounced deshielding, accounting for the downfield shift (δ = 5.47 ppm), whereas the unusual upfield shift of the CH_2 resonance from one of the cyclotridecene units (C14, δ^1H = −0.10 ppm) could arise from shielding effects associated with the anisotropic environment of the Cp ligands (see Fig. S92). As previously noted for complexes **5r** and **5t**, the two cyclotridecene systems adopt a *trans* configuration.

Performing the reaction in *n*-hexane resulted in the formation of complexes **5t** and **5t′**, while the isomerization of the 1,2-allene **t** to the corresponding 1,3-diene **t′** proceeded to a significant extent (Fig. S91). To assess the catalytic performance, the isomerization was monitored by NMR spectroscopy under catalytic conditions. While $Cp_2Ti(\eta^2$-BTMSA) tended to form stable complexes with allene **t**, the sterically more demanding complex $Cp^*_2Ti(\eta^2$-BTMSA) enabled a smooth and selective conversion to the 1,3-diene **t′**, with no detectable titanium-containing byproducts or liberation of the BTMSA ligand (Fig. S96). The reaction was subsequently performed using

Table 4 Selected bond lengths (Å) and angles (°) of complexes **5n–p**, **5r**, and **5t**

Complex	Ti–C_A	Ti–C_D	C_A–C_B	C_A–C_F	C_B–C_C	C_C–C_D	C_D–C_E	C_A–Ti–C_D
5n	2.1890(7)	2.1888(6)	1.5230(9)	1.3494(9)	1.5327(11)	1.5252(9)	1.3488(9)	86.79(2)
5o	2.1715(14)	2.1875(13)	1.5252(19)	1.348(2)	1.536(2)	1.523(2)	1.3439(19)	86.12(5)
5p	2.2047(6)	2.1792(5)	1.5282(8)	1.3552(8)	1.5314(9)	1.5243(8)	1.3535(8)	85.07(2)
5r	2.2063(5)	2.2047(5)	1.5236(6)	1.3483(6)	1.5449(6)	1.5228(6)	1.3480(6)	79.110(18)
5t	2.205(8)	2.205(7)	1.507(10)	1.337(12)	1.528(10)	1.526(10)	1.317(11)	78.4(3)

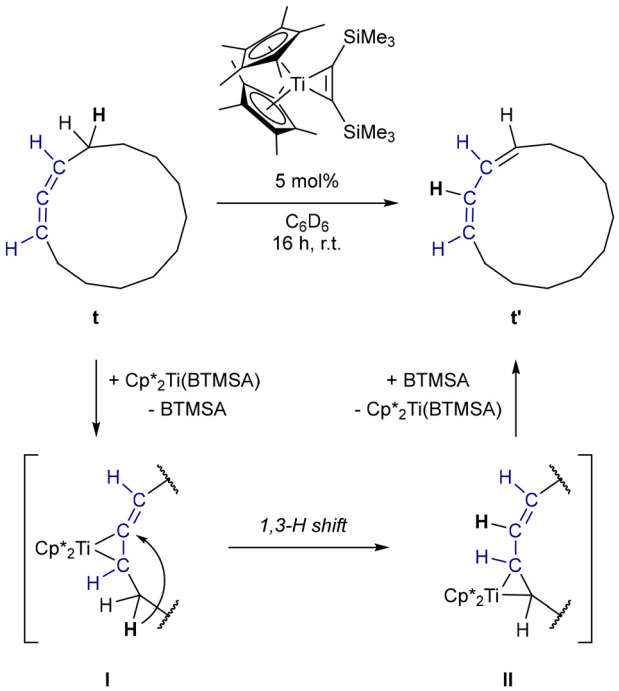

Scheme 6 Titanium-catalyzed isomerization of cyclotrideca-1,2-diene **t** by $Cp^*_2Ti(\eta^2$-BTMSA) yields cyclotrideca-1,3-diene **t′**.

5 mol% of the $Cp^*_2Ti(\eta^2$-BTMSA) catalyst (Scheme 6), demonstrating efficient catalytic turnover under these conditions. This behaviour suggests that the increased steric bulk of the Cp* ligands restricts prolonged coordination of the allene, allowing only transient interaction sufficient to promote the isomerization.

The isomerisation of allenes to 1,3-dienes has been achieved through a variety of strategies, including thermal, acidic, and metal-mediated methods. Early work in the 1960s and 1970s demonstrated that cyclopropyl-substituted allenes can undergo thermal rearrangement, while subsequent studies in the late 1980s reported that allenic systems are capable of forming cyclopentyl dienes at elevated temperatures.[31] Acid-catalysed protocols, employing both mineral acids and organic Brønsted acids, have also been explored; however, these approaches generally show a restricted substrate scope and tend to favour electron-rich allenes.[32] More recently, transition-metal complexes, particularly those of palladium and gold, have been employed to mediate allene rearrangements to 1,3-dienes, highlighting the potential of metal coordination to facilitate these transformations.[33] Given the well-established ability of titanium complexes to form metallacyclic intermediates with unsaturated substrates, we considered that cyclic allenes might undergo analogous activation pathways. Despite this conceptual precedent, to the best of our information, no examples of titanium-mediated isomerization of cyclic allenes to 1,3-dienes have been reported. We propose that allene **t** initially displaces the BTMSA ligand, resulting in a formal oxidative addition at the *in situ* generated $Cp^*_2Ti(II)$ fragment to give olefin complex **I** (Scheme 6). This complex may then undergo a formal 1,3-hydrogen shift, yielding olefin complex **II**. Subsequent reductive elimination is expected to furnish the conjugated 1,3-diene **t′**, while regenerating the $Cp^*_2Ti(\eta^2$-BTMSA) catalyst and completing the catalytic cycle. The transformation is likely driven, at least in part, by relief of ring strain in the cyclic allene. Recoordination of the alkyne ligand BTMSA to the titanium center is facilitated by its favorable π-acceptor properties relative to olefins. Mechanistic studies on 1,3-hydrogen shifts in allenic systems suggest that such rearrangements are electronically feasible, although the precise role of the titanium center in this process remains to be established.[34] Further investigations will also assess the applicability of this catalytic system to a broader range of (cyclic) allenes and provide deeper mechanistic insight into the titanium-mediated 1,3-hydrogen shift.

Conclusions

In summary, this work expands the reactivity profile of Rosenthal's reagent $Cp_2Ti(\eta^2$-BTMSA) **1** toward cyclopropenes and allenes, enabling selective carbon–carbon bond formation under mild conditions. Direct and selective insertion of cyclopropenes afforded bicyclic titanacyclopentenes **2a–d**, whose structures were confirmed by NMR spectroscopy and X-ray diffraction. Controlled rearrangement of **2a–d** afforded the titanacyclobutenes **3a–d** *via in situ* generated titanium carbene intermediates. These intermediates undergo either a [2 + 2] cycloaddition with the BTMSA ligand or react with 1,2-diphenylacetylene to give **4c** and **4d**. The methodology was extended to a broad range of allenes, furnishing diverse titanacyclopentanes **5a–t** through substitution of the BTMSA ligand. For cyclotrideca-1,2-diene **t**, partial isomerization to the corresponding 1,3-diene **t′** was observed, which was further promoted catalytically using $Cp^*_2Ti(\eta^2$-BTMSA). These results highlight a new example of titanium(II)-mediated catalytic isomerization of a strained cyclic allene, illustrating the capacity

of Rosenthal-type complexes to enable both stoichiometric and catalytic transformations. They further underscore the versatility of $Cp_2Ti(\eta^2$-BTMSA) in activating both cumulated and strained π-systems, expanding the known reactivity space of low-valent titanium complexes and providing a foundation for further exploration of Rosenthal-type complexes with unconventional unsaturated substrates.

Author contributions

ME was responsible for the conceptualization, methodology, synthesis, characterization, and preparation of the manuscript. DG was responsible for the synthesis of cyclopropenes and allenes. MS performed the diffraction work. SD and RB supervised the project, acquired the funding, and contributed to the final version of the manuscript.

Conflicts of interest

There are no conflicts to declare.

Data availability

The data supporting this article have been included as part of the supplementary information (SI). Supplementary information: additional experimental details, further spectral and crystallographic data. See DOI: https://doi.org/10.1039/d6dt00059b.

CCDC 2463910–2463915 and 2470638–2470649 contain the supplementary crystallographic data for this paper.[35a–r]

Acknowledgements

Financial support from the DFG Research Training Group 2226 is gratefully acknowledged. Jessica Reimer is thanked for her assistance in synthesizing cyclopropenes and allenes.

References

1 (*a*) H. H. Brintzinger, D. Fischer, R. Mülhaupt, B. Rieger and R. M. Waymouth, *Angew. Chem., Int. Ed. Engl.*, 1995, **34**, 1143–1170; (*b*) L. L. Böhm, *Angew. Chem., Int. Ed.*, 2003, **42**, 5010–5030; (*c*) K. Angermund, G. Fink, V. R. Jensen and R. Kleinschmidt, *Chem. Rev.*, 2000, **100**, 1457–1470.
2 D. Astruc, Olefin Metathesis Reactions: From a Historical Account to Recent Trends, in *Olefin Metathesis*, ed. K. Grela, 2014.
3 (*a*) S. A. Cohen, P. R. Auburn and J. E. Bercaw, *J. Am. Chem. Soc.*, 1983, **105**, 1136–1143; (*b*) M. Fischer, L. Vincent-Heldt, M. Hillje, M. Schmidtmann and R. Beckhaus, *Dalton Trans.*, 2020, **49**, 2068–2072.
4 P. Binger, P. Müller, R. Benn and R. Mynott, *Angew. Chem., Int. Ed. Engl.*, 1989, **28**, 610–611.
5 P. Binger, P. Müller, A. T. Herrmann, P. Philipps, B. Gabor, F. Langhauser and C. Krüger, *Chem. Ber.*, 1991, **124**, 2165–2170.
6 P. Binger, F. Langhauser, P. Wedemann, B. Gabor, R. Mynott and C. Krüger, *Chem. Ber.*, 1994, **127**, 39–45.
7 J. X. McDermott, M. E. Wilson and G. M. Whitesides, *J. Am. Chem. Soc.*, 1976, **98**, 6529–6536.
8 U. Rosenthal, V. V. Burlakov, P. Arndt, W. Baumann and A. Spannenberg, *Organometallics*, 2003, **22**, 884–900.
9 U. Rosenthal, *Eur. J. Inorg. Chem.*, 2019, **2019**, 895–919.
10 (*a*) U. Rosenthal, *ChemistryOpen*, 2019, **8**, 1036–1047; (*b*) U. Rosenthal, *ChemistryOpen*, 2021, **10**, 1234–1243; (*c*) U. Rosenthal, *Chem. Soc. Rev.*, 2020, **49**, 2119–2139.
11 L. Hao and J. F. Harrod, *Inorg. Chem. Commun.*, 1999, **2**, 191–193.
12 K. Schwitalla, Z. Yusufzadeh, M. Schmidtmann and R. Beckhaus, *Inorg. Chem.*, 2024, **63**, 14392–14401.
13 V. V. Burlakov, A. Ohff, C. Lefeber, A. Tillack, W. Baumann, R. Kempe and U. Rosenthal, *Chem. Ber.*, 1995, **128**, 967–971.
14 T. Beweries, M. Haehnel and U. Rosenthal, *Catal. Sci. Technol.*, 2013, **3**, 18–28.
15 M. Haehnel, M. Ruhmann, O. Theilmann, S. Roy, T. Beweries, P. Arndt, A. Spannenberg, A. Villinger, E. D. Jemmis, A. Schulz and U. Rosenthal, *J. Am. Chem. Soc.*, 2012, **134**, 15979–15991.
16 E. P. Beaumier, C. P. Gordon, R. P. Harkins, M. E. McGreal, X. Wen, C. Copéret, J. D. Goodpaster and I. A. Tonks, *J. Am. Chem. Soc.*, 2020, **142**, 8006–8018.
17 X. Shi, S. Li, M. Reiß, A. Spannenberg, T. Holtrichter-Rößmann, F. Reiß and T. Beweries, *Chem. Sci.*, 2021, **12**, 16074–16084.
18 S. Li, M. Schröder, A. Prudlik, X. Shi, A. Spannenberg, J. Rabeah, R. Francke, B. Corzilius, F. Reiß and T. Beweries, *Chem. – Eur. J.*, 2024, **30**, e202400708.
19 (*a*) P. C. Young, M. S. Hadfield, L. Arrowsmith, K. M. Macleod, R. J. Mudd, J. A. Jordan-Hore and A.-L. Lee, *Org. Lett.*, 2012, **14**, 898–901; (*b*) W. M. Sherrill, R. Kim and M. Rubin, *Tetrahedron*, 2008, **64**, 8610–8617.
20 H. Yasuda and A. Nakamura, *Angew. Chem., Int. Ed. Engl.*, 1987, **26**, 723–742.
21 P. Pyykkö and M. Atsumi, *Chem. – Eur. J.*, 2009, **15**, 186–197.
22 A. G. Orpen, L. Brammer, F. H. Allen, O. Kennard, D. G. Watson and R. Taylor, *J. Chem. Soc., Dalton Trans.*, 1989, **12**, S1–S83.
23 F. H. Allen, O. Kennard, D. G. Watson, L. Brammer, A. G. Orpen and R. Taylor, *J. Chem. Soc., Perkin Trans. 2*, 1987, S1–S19.
24 C. McDade and J. E. Bercaw, *J. Organomet. Chem.*, 1985, 281–315.
25 (*a*) S. T. Nguyen, L. K. Johnson, R. H. Grubbs and J. W. Ziller, *J. Am. Chem. Soc.*, 1992, **114**, 3974–3975; (*b*) T. M. Trnka and R. H. Grubbs, *Acc. Chem. Res.*, 2001, **34**, 18–29.

26 (*a*) R. Beckhaus, K.-H. Thiele and D. Ströhl, *J. Organomet. Chem.*, 1989, **369**, 43–54; (*b*) R. Beckhaus, J. Sang, T. Wagner and B. Ganter, *Organometallics*, 1996, **15**, 1176–1187; (*c*) R. Beckhaus, I. Strauß, T. Wagner and P. Kiprof, *Angew. Chem.*, 1993, **105**, 281–283; (*d*) R. Beckhaus, I. Strauß, T. Wagner and P. Kiprof, *Angew. Chem., Int. Ed. Engl.*, 1993, **32**, 264–266.

27 R. J. McKinney, T. H. Tulip, D. L. Thorn, T. S. Coolbaugh and F. N. Tebbe, *J. Am. Chem. Soc.*, 1981, **18**, 5584–5586.

28 E. V. Anslyn and R. H. Grubbs, *J. Am. Chem. Soc.*, 1987, **109**, 4880–4890.

29 P. Pyykkö and M. Atsumi, *Chem. – Eur. J.*, 2009, **15**, 12770–12779.

30 (*a*) J. Cabezas, R. Poveda and J. Brenes, *Synthesis*, 2018, 3307–3321; (*b*) J. Bielefeld, S. Mannhaupt, M. Schmidtmann and S. Doye, *Synlett*, 2019, 967–971; (*c*) M. Rubin and V. Gevorgyan, *Synthesis*, 2004, 796–800; (*d*) I. Erden, W. Cao, M. Price and M. Colton, *Tetrahedron*, 2008, **64**, 5497–5501; (*e*) Z. Zhao, L. Racicot and G. K. Murphy, *Angew. Chem., Int. Ed.*, 2017, **56**, 11620–11623.

31 (*a*) H. Meier and M. Schmitt, *Tetrahedron Lett.*, 1989, **30**, 5873–5876; (*b*) F. Lehrich and H. Hopf, *Tetrahedron Lett.*, 1987, **28**, 2697–2700; (*c*) T. B. Patrick, E. C. Haynie and W. J. Probst, *Tetrahedron Lett.*, 1971, **12**, 423–424; (*d*) M. Jones, M. E. Hendrick and J. A. Hardie, *J. Org. Chem.*, 1971, **36**, 3061–3062; (*e*) R. Bloch, P. Le Perchec and J.-M. Conia, *Angew. Chem., Int. Ed. Engl.*, 1970, **9**, 798–799; (*f*) J. K. Crandall and D. R. Paulson, *J. Am. Chem. Soc.*, 1966, **88**, 4302–4303.

32 (*a*) R. Sanz, D. Miguel, A. Martínez, M. Gohain, P. García-García, M. A. Fernández-Rodríguez, E. Álvarez and F. Rodríguez, *Eur. J. Org. Chem.*, 2010, 7027–7039; (*b*) E. Wenkert, M. H. Leftin and E. L. Michelotti, *J. Org. Chem.*, 1985, **50**, 1122–1124; (*c*) T. L. Jacobs and R. N. Johnson, *J. Am. Chem. Soc.*, 1960, **82**, 6397–6404.

33 Y. Al-Jawaheri, M. Turner and M. Kimber, *Synthesis*, 2018, 2329–2336.

34 A. Basak, S. N. Gupta, K. Chakrabarty and G. K. Das, *Comput. Theor. Chem.*, 2013, **1007**, 15–30.

35 (*a*) CCDC 2463910: Experimental Crystal Structure Determination, 2026, DOI: 10.5517/ccdc.csd.cc2npwz7; (*b*) CCDC 2463911: Experimental Crystal Structure Determination, 2026, DOI: 10.5517/ccdc.csd.cc2npx09; (*c*) CCDC 2463912: Experimental Crystal Structure Determination, 2026, DOI: 10.5517/ccdc.csd.cc2npx1b; (*d*) CCDC 2463913: Experimental Crystal Structure Determination, 2026, DOI: 10.5517/ccdc.csd.cc2npx2c; (*e*) CCDC 2463914: Experimental Crystal Structure Determination, 2026, DOI: 10.5517/ccdc.csd.cc2npx3d; (*f*) CCDC 2463915: Experimental Crystal Structure Determination, 2026, DOI: 10.5517/ccdc.csd.cc2npx4f; (*g*) CCDC 2470638: Experimental Crystal Structure Determination, 2026, DOI: 10.5517/ccdc.csd.cc2nxx0j; (*h*) CCDC 2470639: Experimental Crystal Structure Determination, 2026, DOI: 10.5517/ccdc.csd.cc2nxx1k; (*i*) CCDC 2470640: Experimental Crystal Structure Determination, 2026, DOI: 10.5517/ccdc.csd.cc2nxx2l; (*j*) CCDC 2470641: Experimental Crystal Structure Determination, 2026, DOI: 10.5517/ccdc.csd.cc2nxx3m; (*k*) CCDC 2470642: Experimental Crystal Structure Determination, 2026, DOI: 10.5517/ccdc.csd.cc2nxx4n; (*l*) CCDC 2470643: Experimental Crystal Structure Determination, 2026, DOI: 10.5517/ccdc.csd.cc2nxx5p; (*m*) CCDC 2470644: Experimental Crystal Structure Determination, 2026, DOI: 10.5517/ccdc.csd.cc2nxx6q; (*n*) CCDC 2470645: Experimental Crystal Structure Determination, 2026, DOI: 10.5517/ccdc.csd.cc2nxx7r; (*o*) CCDC 2470646: Experimental Crystal Structure Determination, 2026, DOI: 10.5517/ccdc.csd.cc2nxx8s; (*p*) CCDC 2470647: Experimental Crystal Structure Determination, 2026, DOI: 10.5517/ccdc.csd.cc2nxx9t; (*q*) CCDC 2470648: Experimental Crystal Structure Determination, 2026, DOI: 10.5517/ccdc.csd.cc2nxxbv; (*r*) CCDC 2470649: Experimental Crystal Structure Determination, 2026, DOI: 10.5517/ccdc.csd.cc2nxxcw.